

Supplementary Information (SI)

for

Thermodynamical Investigation in Renewable Block Copolymers based on Poly(lactic acid) and Poly(ethylene azetate)

Rafail O. Ioannidis,^a Panagiotis A. Klonos,^{a,b,*} Zoi Terzopoulou,^{a,c} Nikolaos
Nikolaidis,^a Apostolos Kyritsis,^b and Dimitrios D. Bikiaris^{a,*}

^a *Department of Chemistry, Laboratory of Polymer Chemistry and Technology, Aristotle University of Thessaloniki, GR-541 24, Thessaloniki, Greece*

^b *Department of Physics, National Technical University of Athens, Zografou Campus, GR-15780, Athens, Greece*

^c *Laboratory of Industrial Chemistry, Department of Chemistry, University of Ioannina, GR-45110, Ioannina, Greece*

* *Corresponding authors: pklonos@central.ntua.gr (P.A.K.); dbic@chem.auth.gr (D.N.B.)*

S1. Experimental details

S1.1. Attenuated total reflection Fourier transform infra-red spectroscopy (ATR-FTIR)

An IRTracer-100 spectrophotometer by Shimadzu (Kyoto, Japan) equipped with a QATR™ 10 Single-Reflection ATR Accessory with a Diamond Crystal, was employed to record the ATR-FTIR spectra for all samples, in particular, in the amorphous state of PLA (melted and fast cooled). The samples were prepared in the form of thin films with thickness of approximately 15 μm . The spectra were obtained in absorbance mode and in the spectral region of 500–4.000 cm^{-1} at a resolution of 2 cm^{-1} . A total of 32 co-added scans was collected, while; the obtained spectra were normalized and baseline-corrected before analysis.

S1.2. Differential scanning calorimetry (DSC, TMDSC)

The DSC measurements were performed in a nitrogen atmosphere of high purity, within the temperature range from -100 to 190 $^{\circ}\text{C}$ by means of a TA Q200 calorimeter (TA Instruments, USA). The instrument had been previously calibrated with sapphires for heat capacity and indium for temperature and enthalpy. The samples, ~ 8 mg in mass, were closed in TZero aluminium pans by TA. Upon erasing of samples' thermal history by heating at a temperature well above melting, the samples were subjected to 3 types of measurements (scans), as follows. **Scan 1** – Fast cooling of the melted sample to keep it amorphous ('Jump' command in TA software), followed by a subsequent heating at 10 K/min. **Scan 2** – Cooling of the melted sample at 10 K/min and subsequent heating at 10 K/min. **Scan 3** – Temperature Modulation DSC (TMDSC) of initially amorphous PLA (melt-quenched) in the temperature range from -100 $^{\circ}\text{C}$ to 80 $^{\circ}\text{C}$, upon heating at 2 K/min, with a temperature modulation amplitude of 1 K and modulation period of 1 min.

The crystalline fraction, CF, can be estimated for PLA or PEAz from the comparison (equation S1) of the corresponding enthalpy change, ΔH , of the melt-/cold- crystallization with the bibliographic heat of fusion of 100% crystalline PLA and PEAz ($\Delta H_{100\%}$), respectively, equalling 93 J/g^1 and 160 J/g^2 .

$$CF = \frac{\Delta H}{\Delta H_{100\%}} \quad (S1)$$

S1.3. X-ray diffraction (XRD)

XRD measurements were carried out at room conditions over the 2θ range from 5° to 45° at a scanning rate of $1^\circ/\text{min}$, by means of a MiniFlex II XRD-diffractometer (Chalgrave, Oxford, UK), with Cu K α radiation for crystalline phase identification ($\lambda=0.154$ nm). XRD was performed on semicrystalline samples that had previously undergone melt-crystallization upon cooling at 10 K/min, as in the performed scan 2 in DSC. This protocol was followed to ensure, among others, that the results by the different techniques are comparable with each other.

The XRD results enable the estimation of the crystallinity degree, CF_{XRD} , upon proper analysis³ and the comparison of the total areas of the crystalline diffraction peaks, A_{cryst} , with that of the total diffraction (amorphous halos and crystalline peaks), $A_{XRD,tot}$, according to equation S2.

$$CF_{XRD} = \frac{A_{cryst}}{A_{XRD,tot}} \quad (S2)$$

S1.4. Polarized light microscopy (PLM)

To visualize the semicrystalline morphology of our systems, PLM was employed during melt- and cold- crystallization. Respectively, this was achieved during cooling, at 10 K/min, of the melted samples and during heating at 10 K/min of the initially melted and quenched samples, imitating the thermal scans 2 (cooling) and 1 (heating) of DSC. For PLM, a Nikon Optiphot-2 polarizing light microscope was used, equipped with a Linkam THMS 600 heating stage, a Linkam TP 91 control unit and a Jenoptic ProgRes C10Plus camera were employed, combined with the Jenoptik ProgRes CapturePro software.

S1.5. Broadband dielectric spectroscopy (BDS)

The molecular dynamics of the polymers was assessed employing BDS. The measurements were performed in gas nitrogen atmosphere by means of a Novocontrol BDS setup (Novocontrol GmbH, Germany) on samples of 14 mm in diameter and ~ 100 μm in thickness. The samples were inserted between finely polished brass electrodes forming a sandwich-like capacitor, melted and quenched therein, in order to remain as amorphous as possible. To prevent the electrical contact between the metallic electrodes and to keep the electrodes distance contact, silica spacers (Novocontrol) were employed. The complex dielectric permittivity, $\varepsilon^* = \varepsilon' - i \cdot \varepsilon''$, was recorded isothermally as a function of frequency in the range from 10^{-1} to 10^6 Hz and in the temperature range between -150 and 120 $^\circ\text{C}$ upon heating at steps of 5 and 10 K.

The BDS isothermal spectra of $\varepsilon''(f)$, which are mainly complex, could be analyzed via fitting model functions such as the Havriliak-Negami (HN) function⁴. The HN model is shown in equation S3. One HN term can be fitted to each of the recorded relaxations⁴.

$$\varepsilon^*(f) = \frac{\Delta\varepsilon}{\left[1 + \left(\frac{if}{f_0}\right)^{\alpha_{HN}}\right]^{\beta_{HN}}} + \varepsilon_\infty \quad (\text{S3})$$

In equation 2, $\Delta\varepsilon$ is the dielectric strength, f_0 is a characteristic frequency related to the frequency of maximum dielectric loss, ε_∞ is a value of the real part of the dielectric permittivity (ε') at $f \gg f_0$, α_{HN} is a shape parameter that denoting the width of relaxations times range and, finally, β_{HN} is another shape parameter that evaluates the symmetry of the $\varepsilon''(f)$ peak. When the relaxation is symmetric, i.e., for $\beta_{HN}=1$, the HN equation is practically equal to the Cole-Cole model⁴.

Upon the evaluation of the relaxation peak maxima, f_{max} , for the various temperatures, T , the time scale relaxation map is constructed [$\log f_{\text{max}}(1000/T)$]. Therein, the local relaxations usually follow the Arrhenius behavior (linear, equation S4), wherein, $f_{0,Arrh}$ is a pre-exponential factor and E_{act} is the activation energy.

$$f(T) = f_{0,Arrh} \cdot e^{-\frac{E_{act}}{kT}} \quad (\text{S4})$$

Contrariwise, the segmental relaxations exhibit mainly a ‘curved’ trend of $\log f_{\max}(1000/T)$, which is characteristic of cooperative dynamics⁴. This is mathematical expressed by the Vogel-Fulcher-Tammann-Hesse (VFTH) equation [81,83] (equation S5), wherein, $f_{0,VFTH}$ is a frequency constant, T_0 is the Vogel temperature at which $f_{0,VFTH} \rightarrow 0$. D is the so-called fragility strength parameter⁵.

$$f(T) = f_{0,VFTH} \cdot e^{-\frac{DT_0}{T-T_0}} \quad (S5)$$

D can be used for the calculation of the chains’ fragility index, m_α , via equation S6, upon fixing $f_{0,VFTH}$ to the phonon value of 10^{13} Hz.⁵ m_α is indicative of the chain-chain cooperativity being connected to the cooperativity length, ζ .

$$m_\alpha = 16 + 590/D \quad (S6)$$

Finally, from the extrapolation of the VFTH to the equivalent frequency of DSC (i.e., $f_{\text{eq,DSC}} \sim 10^{-2.8}$ Hz, relaxation time $\tau \sim 100$ s) we may estimate the ‘dielectric glass transition temperature’, $T_{g,\text{diel}}$.

S.2. Additional results

Tables S1-3.

The samples under investigation, values for the overall molar mass, M_n , number of PLA branches, $M_{n,branch}$, estimated molar mass per branch (on average) and characteristic values obtained by DSC and XRD. *Amorphous state*: glass transition temperatures as recorded by conventional DSC (scan 1), T_g , and TMDSC (reversing part of heat capacity, $T_{g,REV}$. Respectively, we have listed the corresponding changes in heat capacity, Δc_p and $\Delta c_{p,REV}$. *Semicrystalline state*: cold crystallization temperature and enthalpy change, T_{cc} and ΔH_{cc} , respectively, melt/hot crystallization temperature and enthalpy change, T_c and ΔH_c , respectively, melting temperature and enthalpy change, T_m and ΔH_m , respectively, and crystalline fraction as estimated by XRD, CF_{XRD} .

Table S1

	DSC scan 2 (fast cooled)												XRD
	cooling		heating										
sample	T_c (°C)	CF_{c1} (wt%)	T_{g1} (°C)	Δc_{p1} (J/g·K)	T_{g2} (°C)	Δc_{p2} (J/g·K)	T_{cc1} (°C)	CF_{cc1} (wt%)	T_{cc2} (°C)	CF_{cc2} (wt%)	T_m (°C)	CF_m (wt%)	CF_{XRD} (%)
PLA	-	-	-	-	54	0.57	-	-	100	52	173	58	52
97.5/2.5	-	-	-	-	48	0.54	-	-	90	43	172	55	38
95/5	-	-	-	-	38	0.55	-	-	81	45	159/163	48	39
90/10	-	-	-51*	-	35	0.51	-	-	72	42	166	56	42
80/20	86	4	-54*	0.08*	28**	0.30**	-26*	1*	60	35	162	55	45
PEAz	-4*	37*	-53*	0.23*	-	-	9*	3*	-	-	42*	49*	-

Notes: (*) the values refer to PEAz, (**) The values are accompanied by high uncertainty

Table S2

sample	TMDSC (fast cooled)			
	PEAz*		PLA	
	$T_{g,rev}$ (°C)	$\Delta c_{p,rev}$ (J/g·K)	$T_{g,rev}$ (°C)	$\Delta c_{p,rev}$ (J/g·K)
PLA	-	-	57	0.64
97.5/2.5	-	-	47	0.50
95/5	-	-	39	0.44
90/10	-	-	35	0.47
80/20	-55*	0.07*	26	0.36
PEAz	-55*	0.22*	-	-

Table S3

sample	DSC scan 1 (cooled at 10 K/min)												XRD CF _{XRD} (%)
	cooling				heating								
	T_{c1} (°C)	CF _{c1} (J/g)	T_{c2} (°C)	CF _{c2} (wt%)	T_{g1} (°C)	T_{g2} (°C)	T_{cc2} (°C)	CF _{cc2} (wt%)	T_{m1} (°C)	CF _{m1} (wt%)	T_{m2} (°C)	CF _{m2} (wt%)	
PLA	-	-	99	21	-	52	111	23	-	-	173	58	39
97.5/2.5	-	-	92	9	-	45	86	30	-	-	171	54	29
95/5	-	-	92	48	-	32*	-	0	-	-	159 [#]	52	25
90/10	-	-	95	42	-55*	25*,&	74	4	29*	6*	166	55	29
80/20	-11*	6*	93 ^{&}	47	-50*	32*,&	-	0	33*	13*	162	59	31
PEAz	12*	43*	-	-	-53*	-	-	0	20/42*	48*	-	-	-

Notes: (*) the values refer to PEAz, (&) not clear/high uncertainty, (#) triple peak

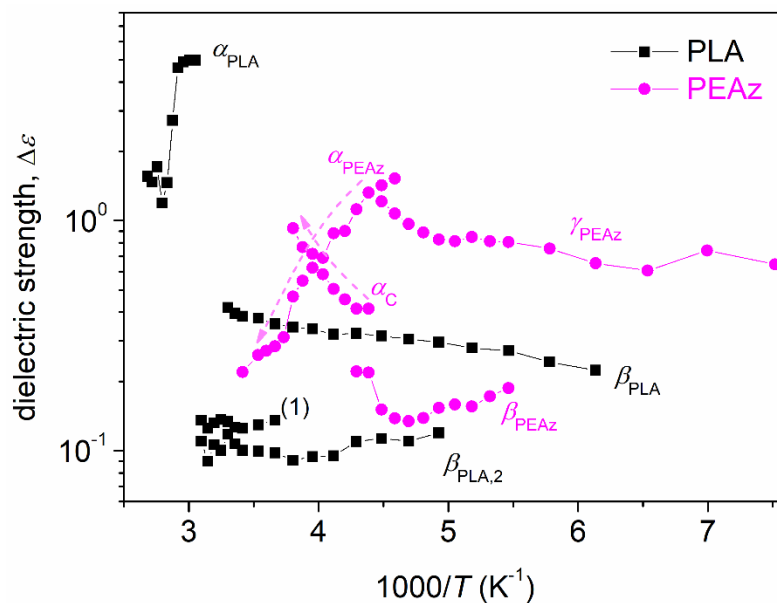


Figure S1. Dielectric strength, $\Delta\epsilon$, as a function of the reciprocal temperature ($1000/T$) for neat PLA and PEAz.

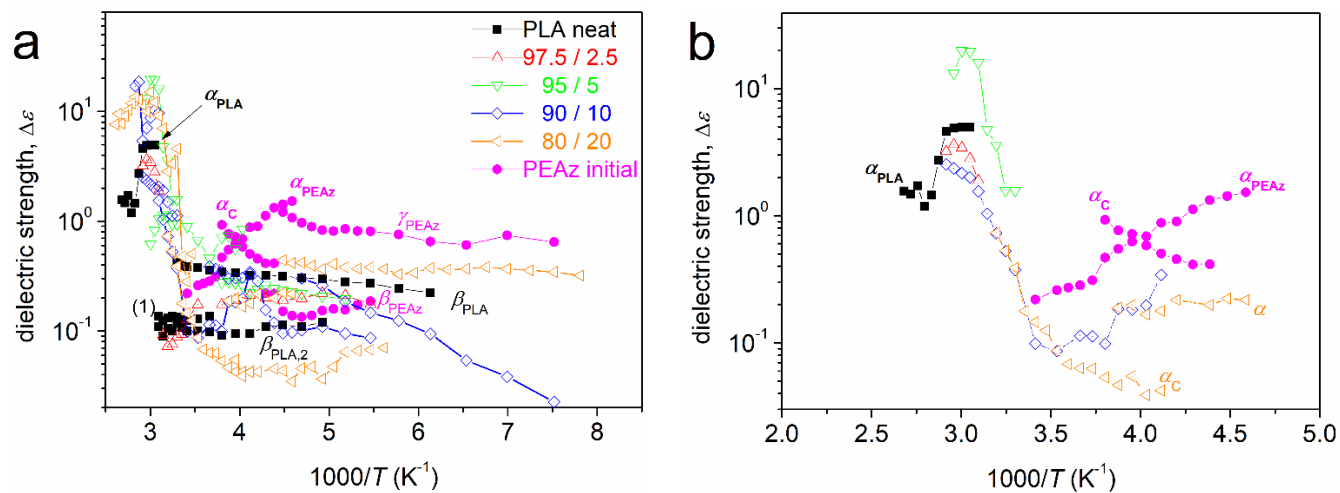


Figure S2. Dielectric strength, $\Delta\epsilon$, as a function of the reciprocal temperature ($1000/T$) for all copolyester compositions and initial PLA and PEAz.

References

1. E.W. Fischer, H.J. Sterzel and G. Wegner, *Kolloid-Zeitschrift und Zeitschrift für Polymere*, 1973, **251**, 980–990.
2. G.Z. Papageorgiou, D.N. Bikiaris, D.S. Achilias and N. Karagiannidis, *Macromol. Chem. Phys.* 2010, **211**, 2585–2595.
3. F. Arai, K. Shinohara, N. Nagasawa, H. Takeshita, K. Takenaka, M. Miya and T. Shiomi, *Polym. J.*, 2013, **45**, 921–928.
4. F. Kremer and F. Schönhals, *Broadband dielectric spectroscopy*, Springer-Verlag, Berlin, 2002.
5. R. Boehmer, K. Ngai, C.A. Angell and D.J. Plazek, *J. Chem. Phys.*, 1993, **99**, 4201–4209.